# Track core size estimation in CR-39 track detector using atomic force microscope and UV-visible spectrophotometer

Yamauchi, Tomoya
Mineyama, Daisuke
Nakai, Hirotake
Oda, Keiji
Yasuda, Nakahiro

revised version: IRaP2002 (O-046)

# Track core size estimation in CR-39 track detector using atomic force microscope and UV-visible spectrophotometer

T. Yamauchi[a,*], D. Mineyama[a], H. Nakai[a], K. Oda[a], N. Yasuda[b]

[a] Kobe University of Mercantile Marine, 5-1-1 Fukaeminami-machi, Higashinada-ku, Kobe 658-0022, Japan.

[b] National Institute of Radiological Science, 4-9-1 Anagawa, Inage-ku, Chiba 263-8555, Japan.

**Abstract**

The radial size of track cores in CR-39 plastics for several types of ions has been determined by two different methods. First, AFM observations were performed on the irradiated CR-39 subsequent to the slight chemical etchings. The track core radii for C, O, Ne and Xe ions evaluated from the intersections of the extrapolated lines, fitted to each growth curve of etch pit radius, were found to be in the range between 2.8 and 4.1 nm, independent of the ion species. Second, UV-visible spectra of the irradiated CR-39 were obtained at various fluences. Based on a track overlapping model, the track core radii are evaluated for H, He, C and O ions. Their core radii were almost proportional to the cube root of the stopping power. The results from the two different measurements are in good agreement with each other.

PACS: 07.79.Lh; 33.20.Lg; 61.80.jh; 61.82.Pv

*Keywords:* Latent track; Track core size; CR-39; AFM; UV-visible spectrum; track overlap

*Corresponding author. Fax +81 78 431 6369; e-mail: yamauchi@cc.kshosen.ac.jp

## 1. Introduction

Among the etched nuclear track detectors, poly-diethylene-glycol bis(allylcarbonate), usually called CR-39, has been one of the most sensitive detectors for more than about 25 years [1]. However, there are some unresolved aspects in the track formation process occurring in this material. Determination of the radial size of the latent tracks in CR-39 is one of most important approaches to an understanding of the track formation mechanism [2].

The conductometric method has been applied to assess the radial track etch rate in various polymers [3-7]. Since the etch rate reflects the radial dose distribution, the method could be useful not only for evaluating the track core size as the first approximation but also for examining the damage distribution around the ion path [8]. On the other hand, FT-IR spectral studies combined with the dose model have been made on cellulose nitrate to estimate the cross section for bond scission [9, 10]. Both methods, which require samples consisting of a thin film, are likely difficult to apply to very brittle CR-39.

As a new imaging tool for etched tracks, the Atomic Force Microscope (AFM) has been demonstrated to have much higher spatial resolution [11-14]. By observing the aperture size of etched tracks after extremely slight etching, the growth curves of the pit radius with nano meter dimension were obtained for fission fragments and several heavy ions [15-17]. Extrapolating the growth curves toward the origin, the coordinates of the intersections were regarded as the track core size. Although this method is similar to the method using SEM [8, 18], it has the great advantage that the surface observations can be made in air without any treatment of the surface. The present authors have also been engaged in spectral studies on CR-39 irradiated by gamma-rays and ions [17, 19-21]. We have revealed that UV spectra of the irradiated CR-39 were sensitively dependent on the absorbed dose and ion fluence, as well as ion species and energy. The fluence dependence of the UV spectra was interpreted as a result of the track overlapping. This means that the track core size in CR-39 can be evaluated from the series of UV spectra based on a suitable model for track overlapping [19, 20].

In the present study, two different methods, namely atomic force microscope and UV-visible spectroscopy, have been applied to estimate the radial size of track cores in CR-39 for light and heavy ions. The results from AFM and UV-visible observations were compared and found to be concordant with each other.

## 2. Materials and experiments

CR-39 of BARYOTRAK (Fukuvi Chemical Ltd., Japan) with thickness 950 μm was utilized in this study. It was made from purified monomers with a degree of purity of more than 99.9%. Calibration data of this material for various light ions have been reported elsewhere [22-24].

The samples for the AFM observation were irradiated by heavy ions, C (8.5MeV), O (8.6MeV), Ne (41.5MeV) and Xe (104MeV), at HIMAC, NIRS, Japan. The irradiations were carried out in air, so the results did not suffer from the vacuum effect in track registration property [25]. The range of fluence was between $10^8$ and $10^9$ ions/cm$^2$, depending on the duration of the subsequent chemical etching. In the other experiment, the samples for the UV-visible observation were irradiated in vacuum at the tandem van de Graaff accelerator at Kobe University of Mercantile Marine. The ions, H (3.4MeV), He (5.1MeV), C (8.5MeV) and O (7.0MeV), were incident normally on CR-39, with higher fluences ranging from $10^{11}$ to $10^{15}$ ions/cm$^2$, where the track overlapping became significant.

The surface observation using AFM was carried out after slight chemical etching in a stirred 6N KOH solution at 70 ºC. The etching duration ranged from 10 to 60 seconds. The 10 seconds etching under this condition corresponds to a thickness of layer removed of about 7 nm provided that the bulk etch rate is constant even in such an extremely near-surface region. Our AFM (OLYMPUS NanoVision 2000, Japan) [17] was operated in the tapping mode using an OLYMPUS Micro Cantilever tip. The UV-visible absorbance was determined with a conventional spectrometer (SHIMAZU Corp., model UV-1600PC) in a room located near to the accelerator [19, 20]. Each measurement was started exactly 5 minutes after exposing the samples to air.

## 3. Results and discussion

### *3.1. Track core radius from AFM method*

The evolution of the pit radius for Xe ions is shown in Fig. 1 as a function of the etching time. The plotted points are the averages over more than 10 measurements of etch pits, and the error bars correspond to the standard deviations. The solid line was attained by a least square fit. As shown in this figure, the first two points seem to have larger values than that expected from the monotonous pit evolution model.

Unfortunately, we do not have enough information on the early stage of the pit growth and the etching property of CR-39 in such a near-surface region to make a more precise consideration on the deviation [17]. Apparently, the fitted line does not pass through the origin. The coordinate of the intersection should represent the track core radius, at which the radial etching rate of the track is significantly increased [15, 16]. From this method, the track core radius of Xe ions was determined to be $r_t = 4.12 \pm 1.6$nm.

Similar behavior of etch pit evolution, namely that the fitted lines do not cross the origin, was observed also for C, O and Ne ions. The deviations of the pit radii at shorter etching times were not significant for these ions. The obtained core radii are summarized in Table 1. The values are in the range between 2.8 and 4.2 and do not depend on the ion species. The stopping power listed in Table 1 was calculated using the StopPow program [26].

*3.2. UV spectra and critical fluence*

All tracks are characterized by a similar chemical structure and radial distribution of color centers. At lower fluences where the track overlapping is negligible, the optical absorbance of the irradiated CR-39 will be simply proportional to the fluence. On the other hand, if overlapping occurs, the optical properties in the overlapped region will be different from those of non-overlapping single tracks. Consequently, absorbance and fluence will no longer be proportional to each other. Using the UV method, the critical fluence, that has been defined as a fluence where the overlapping of tracks becomes significant, was attained from the fluence dependence of UV spectra of the irradiated CR-39 [19, 20].

In Fig. 2, the absorbance at the corresponding wavelength is plotted against the fluence. Below $10^{13}$ ions/cm$^2$, the absorbance at the first peak (240nm) increases proportionally to the fluence. From this diagram, the critical fluence for protons was determined to be about 1.0x10$^{13}$ ions/cm$^2$. From similar diagrams, the critical fluences for He, C and O ions were inferred to be 4.0 x10$^{12}$, 1.0 x10$^{12}$ and 7.0 x10$^{11}$ ions/cm$^2$, respectively. Complete spectral data were given in the literature [19, 20].

*3.3. Track overlapping model*

Let us consider the accumulation process of the tracks in a unit area of 1cm$^2$, each track being expressed by a cylinder whose length is equal to the ion range. In the

top view, the track is a simple circle with an area *s*. Using this assumption, the track accumulation process can be compared with the wetting process of the ground by drops of rain. The area occupied by tracks at a fluence *n* is written as [19, 20]:

$$A(n) = 1 - \exp(-sn). \quad (1)$$

The occupied area consists of regions with different degrees of track overlapping. Eq. (1) can be expanded as

$$A(n) = \{sn\}\exp(-sn) + \left\{\frac{(sn)^2}{2}\right\}\exp(-sn) + \left\{\frac{(sn)^3}{6}\right\}\exp(-sn) + \cdots. \quad (2)$$

The first term on the right side is the area inside tracks without overlapping, the second and third represent the regions of double and triple overlapping, respectively. A derivation of these equations was given in the literature [19, 20].

Because track overlapping is a stochastic process, it does not start at some exact fluence value. Therefore we express the critical fluence as a band with a certain width. We determined that the band starts and ends at the fluences where double and triple overlapping become significant, respectively. The center value of the band was selected as the critical fluence. In this manner, the relation between the critical fluence and the typical track core radius was obtained, as shown in Fig. 3.

*3.4. Track radius evaluated from the AFM and UV methods.*

In Fig. 3, the critical fluences for the examined ions are also shown as vertical bars. For the track core radius of proton, this figure gives us a value of 0.7 nm (0.5-0.95 nm). In the same way, the core radii for He, C and O ion were assessed to be 1.1 nm (0.9-1.6 nm), 2.2 nm (1.8-3.0 nm) and 2.5 nm (2.1-3.5 nm), respectively. The relatively large band of the critical fluence shown in Fig. 3, both borders of the band were given by broken lines, will suppress the uncertainty in the critical fluence cause major problem, that might be derived from the determination step of it.

In Fig. 4, the obtained track core radii are shown as a function of the stopping power for the light ions. The main values of the stopping power are the averaged ones along particle path and the both ends of the error bars are the maximum at the Bragg peaks and the values at the surface. The solid curve is the best fit to the points in the form of the power function, written by,

$$r_t = 0.519\left(\frac{dE}{dx}\right)^{0.39}, \quad \text{in nm}, \quad (3)$$

where *dE/dx* is expressed in units of keV/μm [19, 20]. Some studies have insisted that the core radius in some materials was proportional to the cube root of the stopping power [27, 28]. Further examination for various combinations of ions and materials is necessary to obtain a more general relation between core radius and stopping power.

In Fig. 5, the track core radii from the AFM method in Table 1 are shown as a function of stopping power as well as the extrapolated curve by Eq. (3). The curve was proved experimentally only at lower stopping power regions below 1500 keV/μm by the UV method. The results from the AFM method and the extrapolated curve, however, are in agreement with each other within an experimental error, as shown in this figure.

## 4. Summary

The radial core size of latent tracks in CR-39 plastics for several ions has been studied using AFM and UV-visible spectrophotometer, respectively. AFM observations on the surface of CR-39 irradiated by heavy ions were performed carefully after slight chemical etching. The core radii were evaluated from the growth behavior of minute etch pits. They were in the range between 2.8 and 4.1 nm and hardly dependent on the ion species (C, O, Ne and Xe). On the other hand, UV-visible spectra of ion irradiated CR-39 were obtained as a function of the ion fluence. The track core radii were evaluated from the fluence dependence of the spectra for H, He, C and O ions, based on the model of track overlapping. The core size was found to be almost proportional to the cube root of the stopping power. The results from the two different observations were compared and found to be concordant with each other.

## Acknowledgement

We would like to express our thanks to the staff of NIRS-HIMAC for their support during the experiments (14P138). A part of this work was carried out as a part of the Research Project with Heavy Ions at NIRS-HIMAC.

## References

[1] B.G. Cartwright, E. K. Shirk and P.B. Price, Nucl. Instr. and Meth. 153 (1978) 457.

[2] M.P.R. Waligorski, R.N. Hamm and R. Katz, Nucl. Tracks Radiat. Meas. 11 (1986) 309.

[3] C.P. Bean, M.V. Doyle and G. Entine, J. Appl. Phys. 41 (1970) 1454.

[4] P.Yu. Apel, A. Schulz, R. Spohr, C. Trautmann, V. Vutsadakis, Nucl. Instr. and Meth. B130 (1997) 55.
[5] P.Yu. Apel, A. Schulz, R. Spohr, C. Trautmann, V. Vutsadakis, Nucl. Instr. and Meth. B146 (1998) 468.
[6] P. Apel, R. Spohr, C. Trautmann, V. Vutsadakis, Radiat. Meas. 31, (1999)51.
[7] F. Peterson and W. Enge, Radiat. Meas . 25, (1995) 43.
[8] W. Enge, Radiat. Meas . 25, (1995) 11.
[9] R. Barillon, M. Fromm, A. Chambaudet, R. Katz, J.P. Stoquert and A. Pape, Radiat. Meas . 31, (1999) 71.
[10] R. Barillon and R. Katz, Proc. The First International Symposium on Supercritical Water-cooled Reactors, 406 (2000) 266.
[11] M. Drndic, Y.D. He, P.B. Price, D.P. Snowden-Ifft, and A.J. Westphal, Nucl. Instr. and Meth. B93 (1994) 52.
[12] N. Yasuda, M. Yamamoto, N. Miyahara, N. Ishigure, T. Kanai and K. Ogura, Nucl. Instr. and Meth. B143 (1998) 111.
[13] M. Yamamoto, N. Yasuda, M. Kurano, T. Kanai, A. Furukawa, N. Ishigure and K. Ogura, Nucl. Instr. and Meth. B152 (1999) 349.
[14] N. Yasuda, M. Yamamoto, K. Amemiya, H. Takahashi, A. Kyan and K. Ogura, Radiat. Meas. 31, (1999) 203.
[15] N. Yasuda, K. Uchhikawa, K. Amemiya, N. Watanabe, H. Takahashi, M. Nakazawa, M. Yamamoto and K. Ogura, Proc. The First International Symposium on Supercritical Water-cooled Reactors, 408 (2000) 288.
[16] N. Yasuda, K. Uchhikawa, K. Amemiya, N. Watanabe, H. Takahashi, M. Nakazawa, M. Yamamoto and K. Ogura, Radiat. Meas. 34, (2001) 45.
[17] T. Yamauchi, A. EL-Rahmany, D. Mineyama, H. Nakai and K. Oda, Radiat. Meas. (in press).
[18] L.S. Bohus and E.D. Greaves, Nucl. Tracks Radiat. Meas. 16 (1989) 15.
[19] T. Yamauchi, T. Taniguchi and K. Oda, KEK-Proceedings 99-8 (1999) 45.
[20] T. Yamauchi, H. Ichijo and K. Oda, Proc. The First International Symposium on Supercritical Water-cooled Reactors, 407 (2000) 274.
[21] T. Yamauchi, S. Takada, H. Ichijo and K. Oda, Radiat. Meas. 34, (2001) 69.
[22] T. Yamauchi, K. Oda, S. Tanabe, H. Matsumoto and H. Miyake, Radiat. Meas. 28, (1997) 191.

[23] T. Yamauchi, T. Taniguchi and K. Oda, Radiat. Meas. 31, (1999) 261.
[24] T. Yamauchi, H. Ichiho, K. Oda, B. Doerschel, D. Hermsdorf, K. Kadner, F. Vaginay, M. Fromm and A. Chambaudet, Radiat. Meas. 34, (2001) 37.
[25] T. Yamauchi, K. Oda and H. Miyake, Nucl. Tracks Radiat. Meas. 20, (1992) 615.
[26] B. Doerschel and J. Henniger, Nucl. Instr. and Meth. B171 (2000) 423.
[27] D. Albrecht, P. Armbruster, R. Spohr, M. Roth, K. Schaupert, H. Stuhrmann, Appl. Phys. A37 (1985) 37.
[28] T.A. Tombrello, Nucl. Instr. and Meth. B1 (1984) 23.

Table 1 Track core radius from the AFM method.

| Ion | Energy (MeV) | dE/dx (keV/μm) | Core radius (nm) |
|---|---|---|---|
| C | 8.5 | 995 | 3.64 ± 1.8 |
| O | 8.6 | 1530 | 3.97 ± 1.7 |
| Ne | 41.5 | 1520 | 2.76 ± 1.9 |
| Xe | 104 | 10500 | 4.12 ± 1.6 |

Figure Captions

Fig. 1. The evolution of etch pit in radius for Xe ion (104 MeV) as a function of the etching time.

Fig. 2. Changes in the absorbance at the first (240 nm) and the second (280 nm) peaks of the proton irradiated CR-39.

Fig. 3. Relation between the critical fluence and the track core radius.

Fig. 4. Relation between the track core radius and stopping power.

Fig. 5. Comparison of assessed track core radii from the AFM method and the UV method in CR-39 plastics.

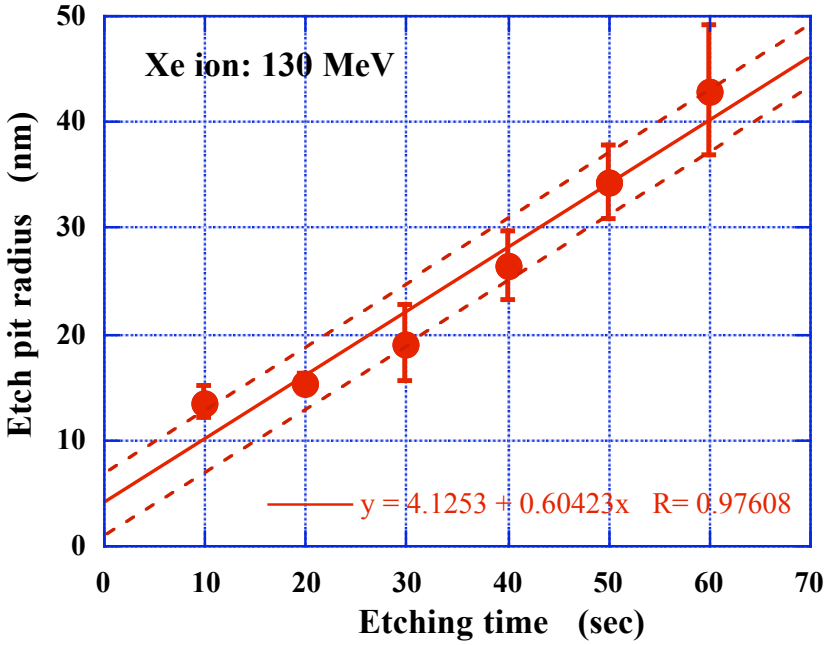


Fig. 1. T. Yamauchi et al.

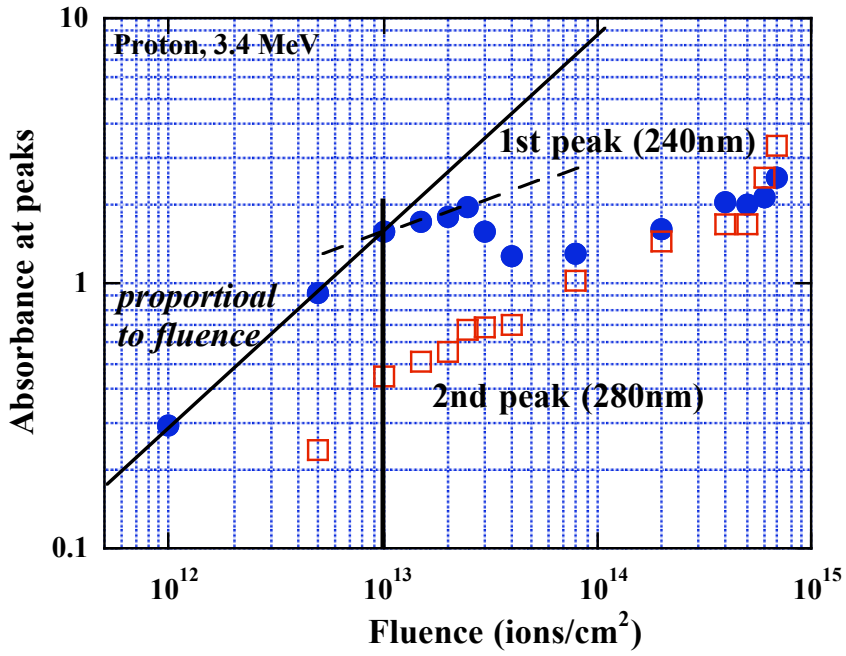


Fig. 2. T. Yamauchi et al.

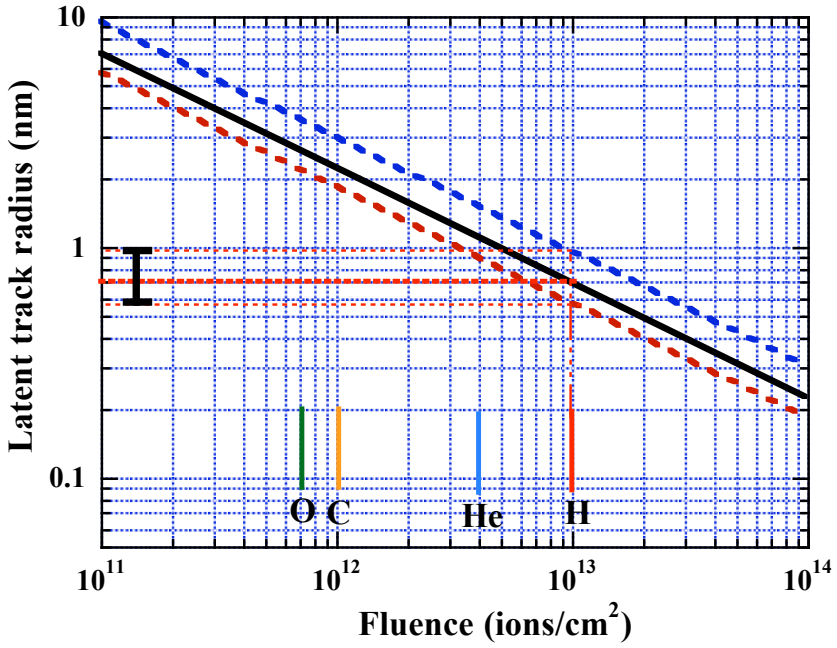


Fig. 3. T. Yamauchi et al.

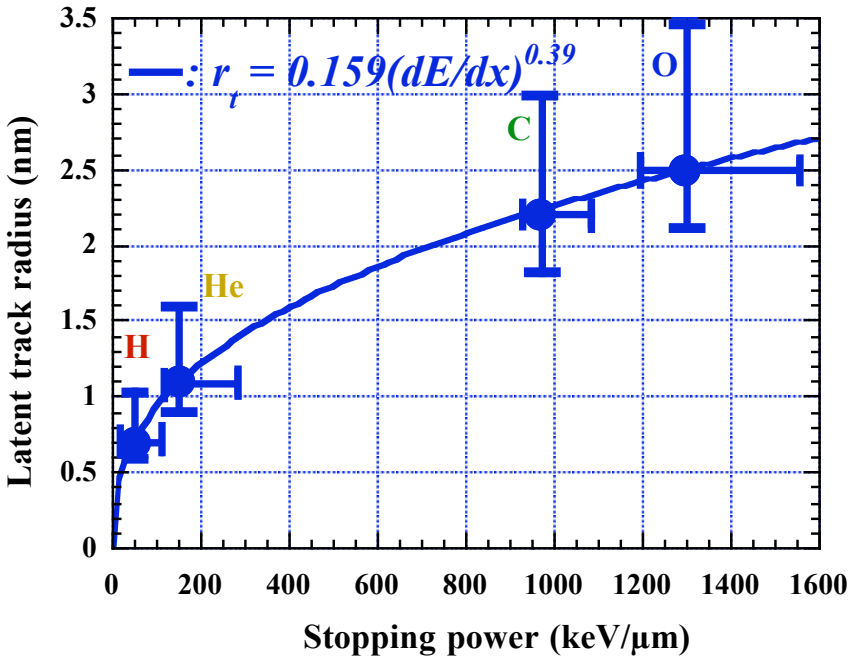


Fig. 4. T. Yamauchi et al.

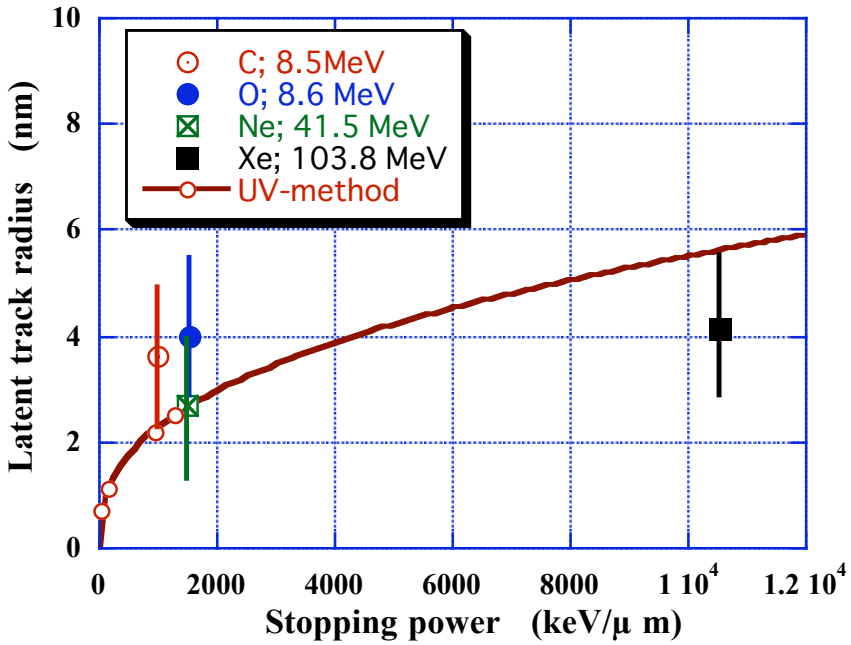


Fig. 5. T. Yamauchi et al.